Materials Today Bio 6 (2020) 100047

Contents lists available at ScienceDirect

Materials Today Bio

journal homepage: www.journals.elsevier.com/materials-today-bio

Enzymatic outside-in cross-linking enables single-step microcapsule production for high-throughput three-dimensional cell microaggregate formation

B. van Loo [a], S.S. Salehi [b], S. Henke [a], A. Shamloo [b,*], T. Kamperman [a], M. Karperien [a], J. Leijten [a,**]

[a] Department of Developmental BioEngineering, Faculty of Science and Technology, Technical Medical Centre, University of Twente, Drienerlolaan 5, 7522, NB Enschede, the Netherlands

[b] School of Mechanical Engineering, Sharif University of Technology, Tehran, Iran

ARTICLE INFO

Keywords:
Cell encapsulation
Droplet microfluidics
Enzymatic cross-linking
Hydrogel
Hollow microgel
Cell spheroid

ABSTRACT

Cell-laden hydrogel microcapsules enable the high-throughput production of cell aggregates, which are relevant for three-dimensional tissue engineering and drug screening applications. However, current microcapsule production strategies are limited by their throughput, multistep protocols, and limited amount of compatible biomaterials. We here present a single-step process for the controlled microfluidic production of single-core microcapsules using enzymatic outside-in cross-linking of tyramine-conjugated polymers. It was hypothesized that a physically, instead of the conventionally explored biochemically, controlled enzymatic cross-linking process would improve the reproducibility, operational window, and throughput of shell formation. Droplets were flown through a silicone delay line, which allowed for highly controlled diffusion of the enzymatic cross-linking initiator. The microcapsules' cross-linking density and shell thickness is strictly depended on the droplet's retention time in the delay line, which is predictably controlled by flow rate. The here presented hydrogel cross-linking method allows for facile and cytocompatible production of cell-laden microcapsules compatible with the formation and biorthogonal isolation of long-term viable cellular spheroids for tissue engineering and drug screening applications.

1. Introduction

The field of microfluidics has emerged as a powerful platform for the manufacturing of advanced micromaterials. The possibility to manipulate liquids using predictable flows allows for the production of cross-linkable droplets with controlled size, shape, and composition for biomedical applications [1–4]. For example, microfluidic droplet generation has been leveraged for the production of hollow core-shell micrometer-sized hydrogels (i.e. microcapsules). The microcapsules' hollow compartment can be used for controlled aggregation of cells into three-dimensional (3D) microtissues such as organoids and microaggregates [5–11].

Cellular microaggregates offer numerous advantages for tissue engineering and drug screening strategies owing to their 3D biomimetic design, which enhances cellular functions in comparison with conventional two-dimensional monolayer cultures [12–14]. For example, microaggregates have been reported to improve stem cell differentiation, facilitate drug target discovery, and enable engineering of macroscopic tissue constructs [15–19]. Cell microaggregates were originally generated using flat non-adherent tissue culture plates, which resulted in microaggregates of polydisperse sizes owing to the lack of geometrical control during the cells' self-assembly process [20]. Consequently, U-shaped multiwell plates [21], conical tubes [22], hanging drops [22], and microwells [18,19,23] have been developed to yield monodisperse spherical microaggregates. However, the inefficient and batch-type nature of these production methods only offered limited quantities of microaggregates, which has hindered their upscaling to industrial and clinical production scales.

In recent years, various microfluidic processes have been explored for the continuous production of monodisperse cell-laden microcapsules [5–11]. Despite significant progress, the microfluidic production of

* Corresponding author.
** Corresponding author.
E-mail addresses: shamloo@sharif.ir (A. Shamloo), jeroen.leijten@utwente.nl (J. Leijten).

https://doi.org/10.1016/j.mtbio.2020.100047
Received 2 January 2020; Received in revised form 18 February 2020; Accepted 19 February 2020
Available online 6 March 2020

microcapsules has remained a complex, inefficient, and labor intensive process, which has hampered its widespread adoption. Specifically, a multistep process has been used in which a sacrificial microgel is produced, coated with distinct biomaterial, and subsequently turned into a microcapsule by enzymatic degradation of the sacrificial core [9,11]. Other methods are, for example, based on multiple emulsion strategies or multistep formation of external shells via layer-by-layer assembly of positively and negatively charged polyelectrolytes [5,7,11]. Moreover, most of these approaches have relied on the ionic cross-linking of alginate, which can be unstable owing to the inherently reversible nature of this physical cross-link and the gradual loss of divalent ions from the cross-linked biomaterial [24]. More straightforward single-step microcapsule production methods have been developed based on competitive enzymatic cross-linking of phenolic compounds. Specifically, tyramine-functionalized polymers droplets can form microcapsules by preventing enzymatic cross-linking of the core using the H_2O_2 (i.e. cross-linking initiator) consuming enzyme catalase [25–27]. Although monodisperse microcapsules were produced in a single cytocompatible step, competitive enzymatic cross-linking remains a delicate biochemical process that depends on balanced activities of cross-linking inducing and inhibiting enzymes, which results in a suboptimal production process (i.e. encapsulation efficiency and shell thickness), restricted level of cross-linking tunability, and limited rate of production. Previously, gradients of H_2O_2-initiated enzymatic cross-linking were observed across semipermeable silicone microfluidic channels [28]. We hypothesized that such cross-linker gradients could be leveraged for the continuous microfluidic formation of microcapsules in the absence of a polymerization inhibitor, thereby providing more control over the reproducibility, operational window, and throughput of microcapsule production than conventional competitive enzymatic cross-linking platforms.

In this study, we present a single-step microfluidic strategy that enabled the high-throughput production of monodisperse hydrogel microcapsules via enzymatic outside-in cross-linking of tyramine-conjugated polymer droplets. Outside-in cross-linking was achieved by supplementing hydrogel precursor droplets with the enzymatic cross-linking initiator H_2O_2 via diffusion through a semipermeable silicone tubing. This method, which involves only a single enzymatic reaction, provided control over the shell thickness and facilitated microcapsule optimization for cell encapsulation. Specifically, dextran-based microcapsules were fine-tuned to enable the cytocompatible encapsulation, aggregation, long-term culture, and on-demand release of mesenchymal stem cells.

2. Results

2.1. Microfluidic platform for diffusion-based delivery of cross-link initiator to microdroplets

A schematic of the microfluidic platform for diffusion-based delivery of the cross-linker to microdroplets is presented in Fig. 1a and b. In short, a 3D microfluidic glass capillary device was manufactured out of

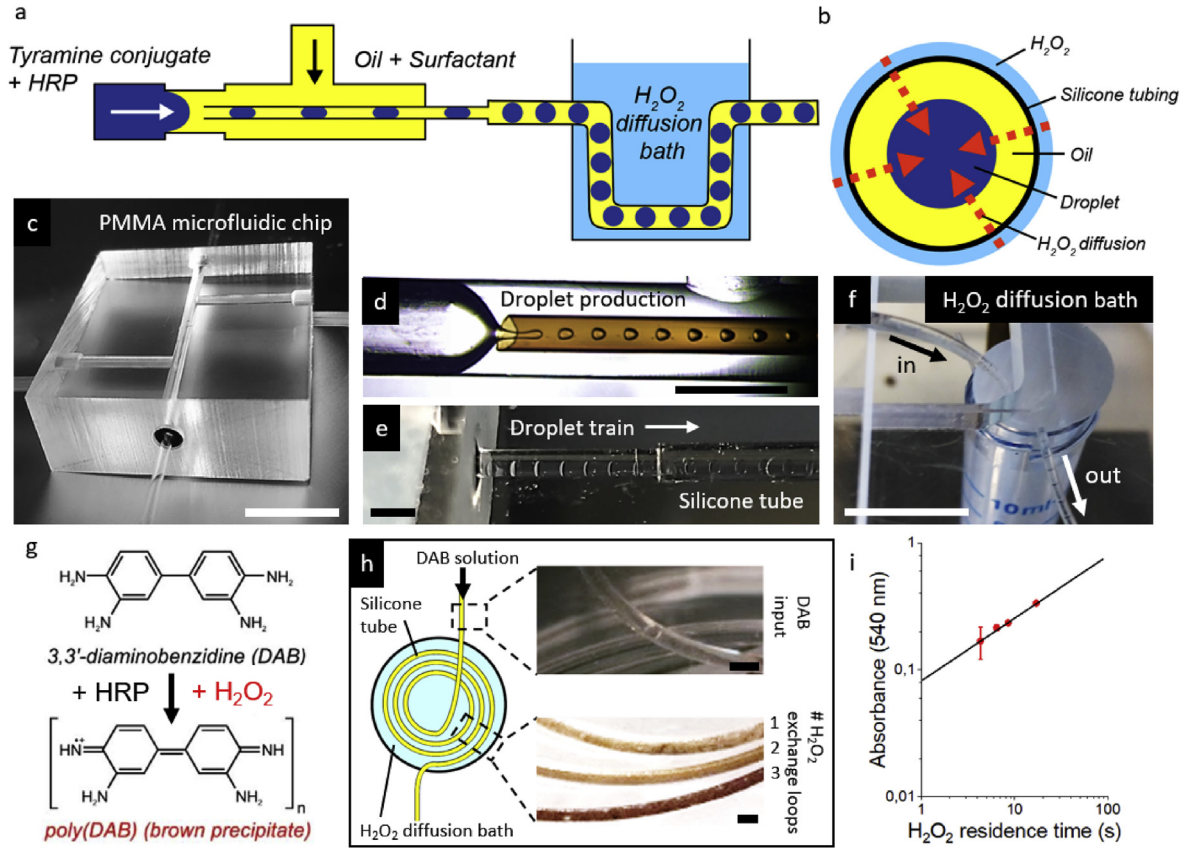

Fig. 1. Microfluidic platform for outside-in diffusion-based delivery of cross-linker to water-in-oil microdroplets. (a) Schematic representation of hydrogel microcapsule production via delayed outside-in cross-linking of water-in-oil polymer microdroplet by transporting the droplets through a silicone tubing submerged in a H_2O_2 bath. **(b)** H_2O_2 diffuses through the silicone tubing, through the oil phase, and into microdroplets. **(c)** Polymethylmethacrylate microfluidic 3D glass capillary device in which **(d)** microdroplets are formed using a flow-focus nozzle setup. **(e)** Droplets are then transported off-chip through a silicone tube, which is **(f)** immersed in a hydrogen peroxide diffusion bath for diffusion of hydrogen peroxide into the droplets. **(g)** DAB forms brown precipitate (poly(DAB)) in presence of HRP and hydrogen peroxide. **(h)** DAB solution was flown through a silicone tube that was immersed in a hydrogen peroxide diffusion bath, which demonstrated the time-dependent nature of the diffusion-based hydrogen peroxide availability. **(i)** Longer hydrogen peroxide residence times resulted in higher absorbance at 540 nm, indicating higher poly(DAB) production and thus higher hydrogen peroxide availability (n = 2). White scale bar indicates 1 cm. Black scale bar indicates 1 mm. DAB, 3,3′-diaminobenzidine; HRP, horseradish peroxidase.

polymethylmethacrylate using a recently reported clean-room independent method to enable the generation of polymer solution droplets (Fig. 1c)[27]. By applying a 1:10 hydrogel precursor:oil ratio at a production flow rate of 100 μl/min while using a 200 μm inner diameter nozzle, droplets were produced at a production rate of approximately 132 Hz (Fig. 2d). Flowing the polymer solution droplets through a semipermeable silicone tube, which was submerged in a hydrogen peroxide bath (Fig. 1e and f), allowed for the diffusion of hydrogen peroxide into the microdroplets.

To prove the diffusion-based delivery of hydrogen peroxide through the silicone tubing, 3,3′-diaminobenzidine (DAB) was used. In the presence of the enzyme horseradish peroxidase (HRP) and hydrogen peroxide, DAB reacts into poly(DAB) which can be observed as a brown precipitate (Fig. 1g). When flowing DAB + HRP solution through a silicone tube submerged in a hydrogen peroxide bath, the formation of brown precipitate was observed, which indicated the diffusion of hydrogen peroxide through the silicone tubing into the solution. Moreover, the quantity of diffused hydrogen peroxide could be predictably controlled as the solution's metachromatic color positively correlated with the solution's residence time in the diffusion bath (Fig. 1h). To validate this finding, microdroplets containing DAB were produced and transported through the hydrogen peroxide diffusion bath with varying residence times. Again, it was observed that longer residence time resulted in a predictable increase in poly(DAB) formation, indicated by the higher absorbance, which was in line with Fick's second law of diffusion. (Fig. 1i).

2.2. Outside-in cross-linking for the production of hydrogel microcapsules

Hydrogels were prepared by the HRP-mediated coupling of phenol moieties of tyramine conjugates (Fig. 2a). As an example material, dextran-tyramine (Dex-TA) was used. Flowing a 5% polymer solution droplets through the submerged silicone tubing for ~8.5 s resulted in the monodisperse production of outside-in cross-linked microgels with a diameter of 123.6 ± 4.9 μm (CV = 3.8) (Fig. 2b). By varying the water:oil ratios and/or different nozzle diameters, microcapsules with diameters ranging from 80 μm to 300 μm could be produced in a monodisperse manner (Fig. 2c and d). Confocal analysis of ethidium homodimer stained microgels confirmed that these microgels were formulated as single core microcapsules (Fig. 2c). To illustrate the possibility to use multiple materials, single core microcapsules were also produced of tyramine-conjugated hyaluronic acid (HA-TA) (Fig. S1).

Control over the local hydrogen peroxide concentration proved to be of essential importance to successfully produce microcapsules using the outside-in cross-linking strategy. When exposing the polymer precursor to a too low hydrogen peroxide concentration it resulted in incomplete cross-linking of microgels' shell (Fig. 2e), which resulted in microgel rupture during the subsequent washing step. Cross-linking the microdroplet with a higher hydrogen peroxide concentration resulted in formation of robust microcapsules (Fig. 2e). Exposure to a too high hydrogen peroxide concentration also resulted in the formation of conformal microcapsules, but associated with the cross-linking of polymer droplet's core thus giving rise to soft-core or solid-core microgels (Fig. 2e). Quantitative analysis of shell thickness and ethidium homodimer intensity of these soft-core microgels confirmed that the polymer cross-linking became gradually less intense in an outside-in manner. This was in contrast to the microcapsules, which revealed a sharp decline in cross-linking density (Fig. 2f).

We then mapped under which parameters partially cross-linked, hollow core, or soft-core microgels would be formed by varying the emulsion's flow rates and the hydrogen peroxide bath's concentration

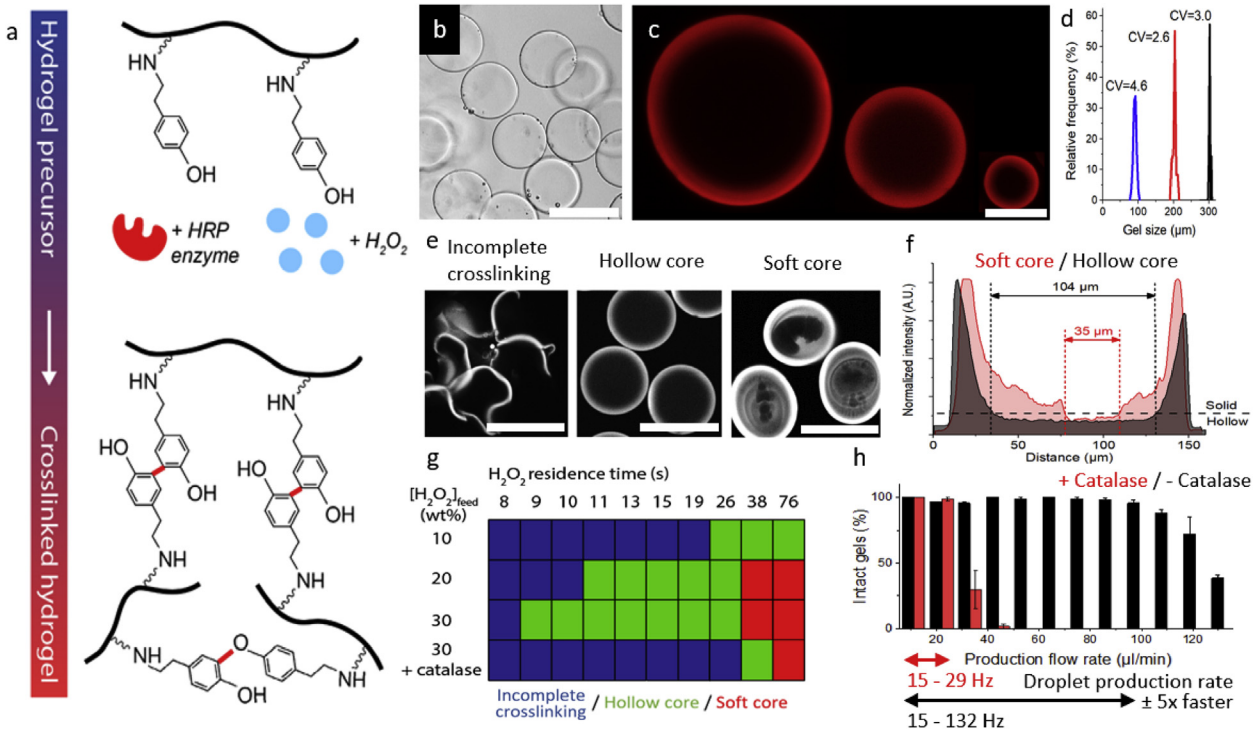

Fig. 2. Outside-In cross-linking of polymer containing water-in-oil microdroplets produces hydrogel microcapsules. (a) Tyramine-conjugated polymer is cross-linked by HRP in the presence of hydrogen peroxide. **(b)** Delayed outside-in cross-linking results in microgels. **(c)** EthD-1 staining proves microgels of different sizes contain a hollow core and can be defined as microcapsules. **(d)** Size distribution of produced microcapsules show monodisperse production in different size regions with a CV < 5 (N ≥ 10). **(e)** Three distinct production regimes, being incomplete cross-linking, hollow microgels, and soft-core microgels, were identified. **(f)** Histogram of soft-core (red) and hollow core microgels (black), with soft-core microgels containing hollow compartments significantly smaller in comparison with the hollow compartments of stable hollow microgels. **(g)** Qualification of Dex-TA cross-linking regime as function of hydrogen peroxide concentration, hydrogen peroxide residence time, and the presence of catalase resulting in incomplete cross-linking (blue), stable hollow microgels (green), and soft-core microgels (red). **(h)** Producing microcapsules without catalase enables higher total flow rates and thus a higher production rate before reaching the incomplete cross-linking regime, as indicated by a low percentage of intact gels (<95%) after cross-linking (N ≥ 20). Scale bar indicates 100 μm. HRP, horseradish peroxidase.

(Fig. 2g, Fig. S2). As expected, decreasing the flow through rate and increasing the hydrogen peroxide concentration associated with increased cross-linking. Microcapsules could be produced at a wide range of emulsion flow rates, which spanned nearly an order of magnitude, with the highest measured microcapsule production rate being measured using an emulsion flow rate of 99 μl/min and a bath concentration of 30% of hydrogen peroxide. This associated with a maximum possible microcapsule production rate of ~132 Hz. In comparison, previously reported catalase-based microcapsule formation strategies based on inside-out hydrogen peroxide scavenging [25], could only form microcapsules in a notably smaller window of operation and at a substantially lower emulsion flow through rate, which offered a maximal microcapsule production rate of only ~29 Hz (Fig. 2g and h). It is likely that delayed outside-in cross-linking can achieve this large production window and higher production, as compared with catalase-based strategies, by avoiding the delicate balance between initiation and inhibition of cross-linking (Table S1). Advantageously, the ability to form microgels using fewer components (e.g. without catalase) not only improves the cross-linking control and rate but also results in a cleaner, more chemically defined production process, which is of relevance for clinical and biomedical applications. In addition, rheological characteristics of the microcapsules can be altered by varying the Dex-TA concentration in the hydrogel precursor solution (Fig. S3).

2.3. Optimization of microcapsules shell thickness for cytocompatible cell encapsulation

As a concrete example for a biomedical application of the presented delayed outside-in cross-linked microcapsule technique, cell encapsulation experiments were performed. Mixing human mesenchymal stem cells (hMSCs) into the hydrogel precursor solution readily allowed for the production of cell-laden microcapsules. However, it was observed that the supplementation of cells to the polymer solution consistently altered the cross-linking of the microdroplets. For example, while cell-free microdroplets produced at a production flow rate of 100 μl/min and cross-linked using a 30% hydrogen peroxide concentration yield hollow microgels, microdroplets containing $2*10^7$ cells/ml resulted in the production of soft-core microgels (Fig. 3a and b). We then demonstrated that cell-laden microdroplets required higher production flow rates than their cell-free counterparts to form microcapsules (Fig. 3a). Advantageously, this allowed for the production of microcapsules at emulsion flow through rates as high as 180 μl/min (Fig. 3c), which resulted in thinner shells with a thickness of 16.7 ± 2.7 μm (Fig. 3d). This increased flow rate equates to a production rate of ~230 Hz, which is almost double the maximum production rate of cell-free microcapsules, and ~8× faster than catalase-dependent microcapsule production.

The microgel's shell thickness is of great importance for cell encapsulation as it positively correlates with cells becoming entrapped in the shell. Moreover, although cell death was negligible within the hollow compartment, it was observed that cell death of entrapped cells in the shell was relatively high (Fig. 3e) being 67 ± 5% after 14 days of culture. However, by adjusting the production flow rate from 100 μl/min to 180 μl/min we were able to lower the amount of entrapped cells from 15% to 0,2% (Fig. 3f) effectively optimizing the cytocompatible cell encapsulation within the microcapsules.

The number of encapsulated cells could be controlled by tuning the cell concentration in the hydrogel precursor solution. For example,

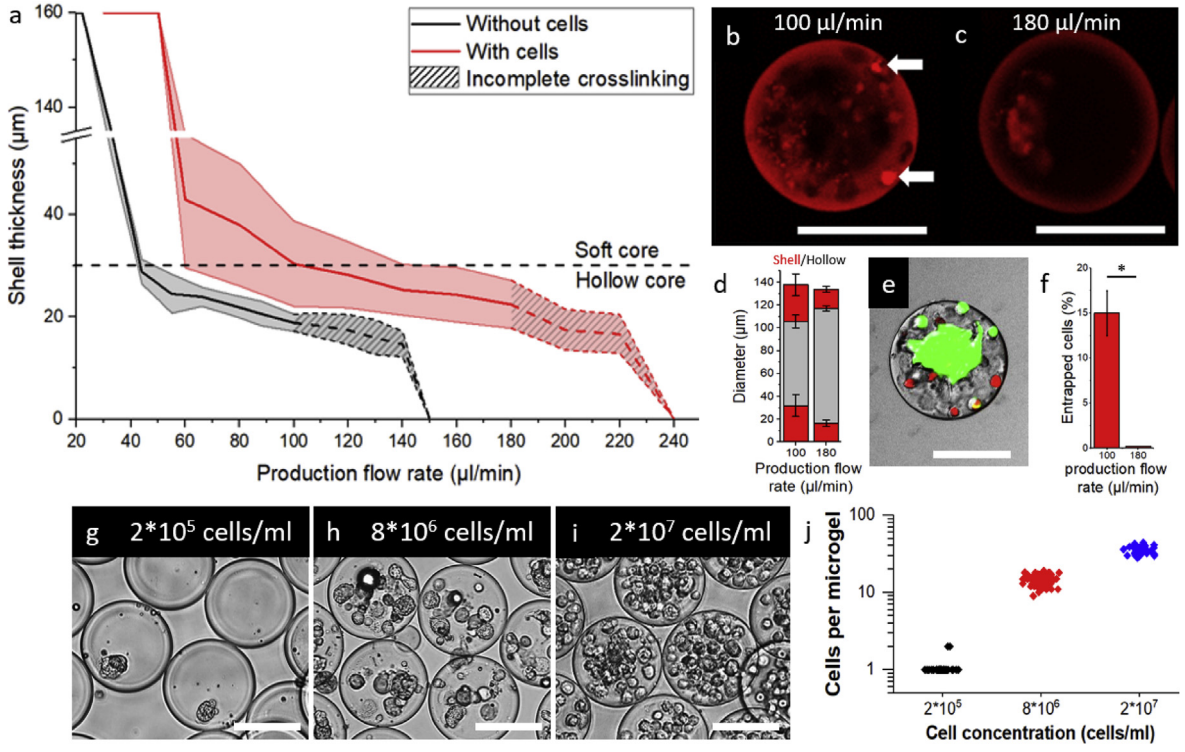

Fig. 3. Optimization of microcapsules shell thickness for efficient cell encapsulation. (a) Quantification of shell thickness at different production flow rates with and without $2*10^7$ of hMSCs in the polymer solution. (N ≥ 20). **(b)** Cell-laden microcapsules produced at a production flow rate of 100 μl/min resulted in soft-core microgels with cell entrapment in the shell, as indicated by white arrows **(c)** Cell-laden hollow core microcapsules were obtained when produced with a production flow rate of 180 μl/min. **(d)** Shell size decreases with increasing production flow rates (N ≥ 15). **(e)** Live/dead assay of cell-laden microcapsules showed that dead cells (shown in red) tend to be entrapped in the microgel's shell. **(f)** Number of cells entrapped in the shell drop from 15% to 0.2% with higher production flow rates. **(g)** Cell encapsulation with a cell concentration of $2*10^5$ cells/ml in the hydrogel precursor solution for single-cell encapsulation. Further increasing the cell concentration in the polymer solution to **(h)** $8*10^6$ or **(i)** $2*10^7$ cells/ml resulted in the encapsulation of a predictable amount of multiple cells. **(j)** Quantification of the number of cells per microcapsule for different cell concentrations in the hydrogel precursor solution (N ≥ 30). Scale bar indicates 100 μm * Indicates significance with $p < 0.05$. hMSCs, human mesenchymal stem cells.

single-cell hollow microcapsules were produced using a concentration of $2*10^5$ cells/ml (Fig. 3g). Specifically, a single cell was present in 35% of the microcapsules, whereas only 2% of the hollow microgels contained two or more cells. This strategy thus represents an effective approach to study individual cells within soft, hollow, and 3D microenvironments, which can be composed of spatiotemporally responsive materials [29].

The number of cells per microgel scaled in a predictable manner with the cell concentration used in the hydrogel precursor solution, which thus also enabled the production of microcapsules that contained multiple cells (Fig. 3h and i). Delayed outside-in cross-linking of 120 μm diameter microdroplets composed of $2*10^7$ cells/ml polymer solution resulted in the monodisperse encapsulation of 34.4 ± 3.1 cells per microcapsule (CV = 9.2%). Increasing the cell concentration further associated with a linear increase in the number of encapsulated cells within the microcapsule, which corroborated the predictable nature of the encapsulation process (Fig. 3j). Besides the cell concentration in the hydrogel precursor solution, the amount of cells per microcapsule could also be tuned by producing microcapsules of different sizes. For example, production of microcapsules of 298 ± 9 μm resulted in 101 ± 8 cells per gel (Fig. S4).

2.4. Long-term culture of cell-laden microcapsules enable in situ formation of stem cell–based 3D microtissues

The semipermeable nature of the microcapsules was studied with diffusion experiments using fluorescein isothiocyanate-conjugated dextrans of various molecular weights, which illustrated that molecules up to 150 kDa were are able to diffuse into the microcapsule (Fig. S5). Relevant molecules such as growth factors, nutrients and waste products, can thus diffuse freely through the microcapsules' shell. This indicated that long-term cell culture is most likely possible within the microcapsules.

hMSC containing microcapsules were produced and cultured for up to 28 days (Fig. 4a–c). Cells rapidly aggregated into 3D microtissues within the hollow compartment of the microcapsules. These microaggregates could be maintained within the microcapsules for the entire duration of experimentation without any notable level of cell egression. As with conventionally cultured stem cell microaggregates, the cellular spheroids decreased (e.g. 62% reduction in 28 days) in diameter over time (Fig. 4d) [19,23]. This observation is likely explained by cellular compaction within the microaggregate, as previously reported [18], as cell viability consistently remained high directly after encapsulation and after a culture period of 28 days in multiple experiments (n = 4), with a viability of 86 ± 1% 5 h after encapsulation and 83 ± 7% of cells surviving after 28 days of culture (Fig. 4e, Fig. S6). This indicated that the diffused hydrogen peroxide was offered to the cell-laden microdroplet in a non-toxic concentration as the hydrogen peroxide–free syringe control associated with a comparable level of cell survival. This was likely mediated via the outside-in consumption of hydrogen peroxide during the cross-linking reaction, which effectively shielded the cells in the droplets core from exposure to cytotoxic levels of hydrogen peroxide. This emphasized the cytocompatible nature of the delayed outside-in cross-linking process. Moreover, fluorescent confocal analysis revealed that the microfluidic encapsulation procedure prevented cells from being at the peripheral side of the microcapsules, thus effectively locating the cells within the microcapsules core and allowing the formation of conformal and continuous shells (Fig. 4f). Interestingly, evidence was found that cells could originally reside on the proximal side of the microcapsule's shell and vacate their position after cross-linking. (Fig. 4g). Furthermore, enzymatic digestion of the Dex-TA microcapsules using dextranase allowed for biorthogonal isolation of the produced microaggregates (Fig. 4h).

3. Discussion

Here, we present a robust and straightforward method to produce hydrogel-based hollow single-core microcapsules. Our method relies on the enzymatic cross-linking of polymer-tyramine conjugates in an enzymatic reaction that is cytocompatible, achieved in seconds, and controlled via outside-in diffusion of a cross-link activator (e.g. hydrogen peroxide). By exposing polymer solution microdroplets to outside-in diffusion of low amounts of hydrogen peroxide, which can be controlled by adjusting the production flow rate, hydrogen peroxide

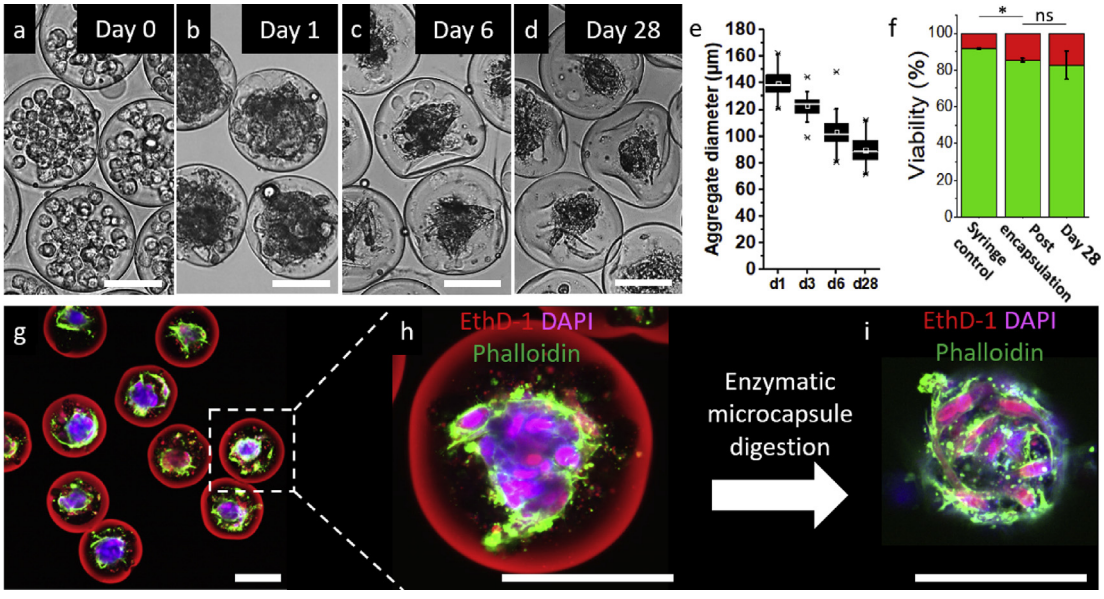

Fig. 4. Cell-laden microcapsules enable in situ formation, formation, and biorthogonal isolation of stem cell based 3D microtissues. Encapsulated cells in microcapsules (a) immediately after cross-linking, **(b)** after 1 day of culture, **(c)** after 6 days of culture, **(d)** and after 28 days of culture. **(e)** Quantification of the size of the microtissues formed within the microcapsules. **(f)** Quantification of live/dead assays of used hMSCs at various point in time (N ≥ 20). **(g)** Confocal images of microaggregates in microcapsules after 14 days of culture, stained with EthD-1 (red), DAPI (magenta), and Phalloidin (green). **(h)** High resolution confocal microphotograph of a single microaggregate in a microcapsule after 14 days of culture. **(i)** Enzymatic degradation of Dex-TA microgels using dextranase allowed for biorthogonal microaggregate isolation. Scale bar represents 100 μm * Indicates significance with $p < 0.05$. 3D, three-dimensional; hMSCs, human mesenchymal stem cells.

concentration and possibly by varying the thickness of the silicone tubing, microcapsules are effectively formed as the hydrogen peroxide will be consumed in the cross-linking reaction before being able to reach the microdroplet's core.

Compared with previously reported strategies, such as those based on the spatial competition between an inducer (e.g. hydrogen peroxide) and an inhibitor (e.g. catalase) of polymer cross-linking [25], our system offers several advantages that are a consequence from its activator--only–based design. Specifically, it is a cleaner, more chemically defined production process, which is favorable when taking possible future clinical studies into account. In addition, as no inhibitors are used, the microcapsules could be produced at a substantially higher production rate while offering a wider window of operation. Furthermore, as our system relies on delayed cross-linking, the cross-linking of polymer at the droplet generator's nozzle is avoided, which lowers the chance on microdevice failure [27]. Moreover, several other previously published methods described for production of microcapsules demand access to nano and microfabrication technologies and dedicated infrastructures, whereas our method relies on the use of off-the-shelve components and readily available non–clean-room–based production processes, thus being suitable for a much wider target audience as it includes non-specialized end-users [27].

The enzymatic cross-linking of Dex-TA has been used for various biomedical applications and can be combined with distinct production techniques [26–32]. Dex-TA is thus chosen as a model material as it represents an effective, versatile, inert, and cytocompatible biomaterial. Regardless, the presented method for microcapsule production is compatible with a wide variety of polymers. Numerous natural and synthetic tyramine polymer conjugates to form hydrogel networks have previously been reported. Beside Dex-TA, conjugates of hyaluronic acid [32], poly(ethylene glycol) [33], heparin [31], chitosan [34], alginate [35], gelatin [36], Poly Vinyl Alcohol [37], and peptides [38] have been reported. These conjugates and their combination thereof, each with their own biological and physicochemical properties, are all suited for outside-in enzymatic cross-linking. Hence, it will be possible to tailor the biological and physicochemical properties of the microcapsule's shell by selecting distinct polymer conjugates and stimulating moieties. To demonstrate this, microcapsules consisting of different concentrations of Dex-TA and HA-TA were produced as described earlier.

Encapsulating cells using outside-in cross-linking associated with excellent cell survival, despite the silicone delay line being submerged in a bath composed for 30% of hydrogen peroxide. Indeed, it is widely known that too high concentrations of hydrogen peroxide cause acute cell death [39]. However, it is also known this cytotoxicity depends on both dose and incubation time. For example, decreasing the H_2O_2 concentration from 500 to 30 μm required, respectively, 1 h and 48 h to show cytotoxic effects [40]. In contrast, in our enzymatically cross-linking system, H_2O_2 is rapidly consumed (seconds) and thus allow for extremely short incubation times. Extensive research has shown that these extremely short H_2O_2 exposure times allow for high cell viability and long-term cell function without any detectable functional effect [30,31,34,41–43]. In fact, it was recently demonstrated that our enzymatic cross-linking material system was more cytocompatible than any of the previously studied material systems used for microfluidic generation of microgels [30]. Moreover, the amount of hydrogen peroxide that diffuses through the silicone tubing, through the continuous oil phase, and into the polymer droplet is both limited and controlled and is rapidly consumed by the enzyme HRP to cross-link the polymer into a macromolecular network. Within a few micrometer of diffusion into the microdroplet, the H_2O_2 has decreased to such a low level that it was no longer able to cross-link the microdroplet into a microgel, hence the formation of hollow microcapsules. Consequently, the levels of H_2O_2 within the bulk/core of the microdroplets — where the cells reside — are well within the cytocompatible level. This logic is substantiated by our viability experiments that allowed high cell survival after encapsulation and long-term cell culture. Advantageously, owing to hydrodynamic focusing of microparticles (e.g. cells) inside of aqueous solution (e.g. polymer microdroplets), the cells are transported away from the droplet's shell and toward its core [41]. Indeed, using the delayed cross-linking strategy, no cell were present in the peripheral side of the microcapsules' shell, which likely contributed to the excellent postencapsulation survival rates by spatially shielding it from the outside-in diffusing hydrogen peroxide.

When cells were encapsulated, the microcapsules functioned as microbioreactors that enabled the formation of monodisperse 3D microtissues via cellular aggregation. This phenomenon occurs when cell-cell interactions are energetically more favorable as compared with the cell-substrate interactions, which thus requires biomaterials that present little or no cell binding motives. Controllably producing 3D microtissue has numerous application to, amongst others, study a variety of diseases, guide the differentiation of stem cells, and function as microbuilding blocks in bottom-up tissue engineering [16,18–20]. Not surprisingly, several strategies have been developed to facilitate controlled cell microaggregation, which includes microwells, hanging drops, non-adhesive culture substrates [23]. Although being compatible with low throughput academic research, none of these platforms offers a production throughput that is readily suitable for clinical or industrial translation. Moreover, in many of these platforms, long-term cultures need to be protected from aggregate fusing or culture substrate attachment. In addition, changing media in many of these platforms is not a straightforward or facile exercise. Hydrogel microcapsules can overcome these challenges by allowing for facile culture and handling of 3D encapsulated microaggregates, which can be produced in a high--throughput manner. In addition, the biorthogonal isolation of the microaggregates allows for easy analysis and further downstream use of these microtissues.

Although the focus of this study was to produce microcapsules, we also identified regimes where soft-core microgels were produced using outside-in cross-linking of tyramine-conjugated polymers. These systems offer cells to be encapsulated in a soft 3D microenvironment, while being protected from undesired physical such as shear stress and/or compression. Moreover, it offers control over diffusion rates in a manner that is not directly dependent on the hydrodynamic properties of the microgels soft-core but rather on those of the microgel's protective shell. In addition, the shell can mitigate or prevent the cell egression that often challenge the culture of cells in soft microgels [41]. Soft-core microgels therefore represent an interesting tool for studying cell biology, development processes, and pathologies such as cancer. Importantly, as with the microcapsules, the soft-core microgels can be produced in high--throughput, which enables the drug screening using compound libraries [6,44,45].

4. Conclusion

In summary, delayed outside-in cross-linking is an effective, predictable, cytocompatible, universal, and high-throughput strategy for the formation of long-term viable 3D microtissues (e.g. stem cell microaggregates) that allows for biorthogonal purification for downstream biomedical applications such as tissue engineering and drug screening.

Experimental section

A detailed experimental section can be found in the Supporting Information.

Supporting information

Supporting Information is available from the publisher or from the author.

Author contributions

Conception by SH, TK and JL. Experimental design by BvL, SS, TK and JL. Data interpretation by all authors. Manuscript written by BvL, TK and

JL. Supervision and revisions by AS, MK and JL.

Declaration of competing interest

The authors declare that they have no known competing financial interests or personal relationships that could have appeared to influence the work reported in this paper.

Acknowledgements

J.L. acknowledges financial support from an Innovative Research Incentives Scheme Vidi award (#17522) from the Netherlands Organization for Scientific Research (NWO), the European Research Council (ERC, Starting Grant, #759425), and the Dutch Arthritis Foundation (#17-1-405). A.S. acknowledges financial support from Iran National Science Foundation: INSF (#95827599).

Appendix A. Supplementary data

Supplementary data to this article can be found online at https://doi.org/10.1016/j.mtbio.2020.100047.

References

[1] E. Kang, G.S. Jeong, Y.Y. Choi, K.H. Lee, A. Khademhosseini, S.-H. Lee, Digitally tunable physicochemical coding of material composition and topography in continuous microfibres [Internet], Nat. Mater. 10 (2011 Sep 4) 877, https://doi.org/10.1038/nmat3108. Available from:.

[2] S. Ma, J. Thiele, X. Liu, Y. Bai, C. Abell, W.T.S. Huck, Fabrication of microgel particles with complex shape via selective polymerization of aqueous two-phase systems [Internet], Small 8 (15) (2012 May 31) 2356–2360, https://doi.org/10.1002/smll.201102715. Available from:.

[3] G.M. Whitesides, The origins and the future of microfluidics [Internet], Nature 442 (2006 Jul 26) 368, https://doi.org/10.1038/nature05058. Available from:.

[4] S. Xu, Z. Nie, M. Seo, P. Lewis, E. Kumacheva, H.A. Stone, et al., Generation of monodisperse particles by using microfluidics: control over size, shape, and composition [Internet], Angew. Chemie. Int. Ed. 44 (5) (2005 Jan 18) 724–728, https://doi.org/10.1002/anie.200462226. Available from:.

[5] P. Agarwal, S. Zhao, P. Bielecki, W. Rao, J.K. Choi, Y. Zhao, et al., One-step microfluidic generation of pre-hatching embryo-like core-shell microcapsules for miniaturized 3D culture of pluripotent stem cells, Lab Chip 13 (23) (2013 Dec) 4525–4533.

[6] K. Alessandri, B.R. Sarangi, V.V. Gurchenkov, B. Sinha, T.R. Kiessling, L. Fetler, et al., Cellular capsules as a tool for multicellular spheroid production and for investigating the mechanics of tumor progression in vitro, Proc. Natl. Acad. Sci. U. S. A. 110 (37) (2013 Sep) 14843–14848.

[7] Q. Chen, S. Utech, D. Chen, R. Prodanovic, J.-M. Lin, D.A. Weitz, Controlled assembly of heterotypic cells in a core–shell scaffold: organ in a droplet [Internet], Lab Chip 16 (8) (2016) 1346–1349, https://doi.org/10.1039/C6LC00231E. Available from:.

[8] C. Kim, S. Chung, Y.E. Kim, K.S. Lee, S.H. Lee, K.W. Oh, et al., Generation of core-shell microcapsules with three-dimensional focusing device for efficient formation of cell spheroid, Lab Chip 11 (2) (2011 Jan) 246–252.

[9] S. Sakai, S. Ito, Y. Ogushi, I. Hashimoto, N. Hosoda, Y. Sawae, et al., Enzymatically fabricated and degradable microcapsules for production of multicellular spheroids with well-defined diameters of less than 150 microm, Biomaterials 30 (30) (2009 Oct) 5937–5942.

[10] L. Yu, C. Ni, S.M. Grist, C. Bayly, K.C. Cheung, Alginate core-shell beads for simplified three-dimensional tumor spheroid culture and drug screening, Biomed. Microdevices 17 (2) (2015 Apr) 33.

[11] C.R. Correia, I.M. Bjørge, J. Zeng, M. Matsusaki, J.F. Mano, Liquefied microcapsules as dual-microcarriers for 3D+3D bottom-up tissue engineering [Internet], Adv. Healthc. Mater. 8 (22) (2019 Nov 1) 1901221, https://doi.org/10.1002/adhm.201901221. Available from:.

[12] K.A. Fitzgerald, M. Malhotra, C.M. Curtin, F.J. O' Brien, C.M. O' Driscoll, Life in 3D is never flat: 3D models to optimise drug delivery [Internet], J. Control Release vol. 215 (2015) 39–54. Available from: http://www.sciencedirect.com/science/article/pii/S016836591530033X.

[13] B.M. Baker, C.S. Chen, Deconstructing the third dimension – how 3D culture microenvironments alter cellular cues [Internet], J. Cell Sci. 125 (13) (2012 Jul 1) 3015. LP – 3024. Available from: http://jcs.biologists.org/content/125/13/3015.abstract.

[14] E.R. Shamir, A.J. Ewald, Three-dimensional organotypic culture: experimental models of mammalian biology and disease [Internet], Nat. Rev. Mol. Cell Biol. 15 (2014 Sep 17) 647, https://doi.org/10.1038/nrm3873. Available from:.

[15] Y.T. Matsunaga, Y. Morimoto, S. Takeuchi, Molding cell beads for rapid construction of macroscopic 3D tissue architecture [Internet], Adv. Mater. 23 (12) (2011). H90–4. Available from: https://onlinelibrary.wiley.com/doi/abs/10.1002/adma.201004375.

[16] C.R. Thoma, M. Zimmermann, I. Agarkova, J.M. Kelm, W. Krek, 3D cell culture systems modeling tumor growth determinants in cancer target discovery [Internet], Adv. Drug Deliv. Rev. 69 (70) (2014) 29–41. Available from: http://www.sciencedirect.com/science/article/pii/S0169409X14000350.

[17] O.I. Hoffmann, C. Ilmberger, S. Magosch, M. Joka, K.-W. Jauch, B. Mayer, Impact of the spheroid model complexity on drug response [Internet], J Biotechnol 205 (2015) 14–23. Available from: http://www.sciencedirect.com/science/article/pii/S0168165615000917.

[18] J. Bolander, W. Ji, J. Leijten, L.M. Teixeira, V. Bloemen, D. Lambrechts, et al., Healing of a large long-bone defect through serum-free in-vitro priming of human periosteum-derived cells [Internet], Stem Cell Rep. 8 (3) (2017 Mar 14) 758–772, https://doi.org/10.1016/j.stemcr.2017.01.005. Available from:.

[19] J. Leijten, L.S.M. Teixeira, J. Bolander, W. Ji, B. Vanspauwen, J. Lammertyn, et al., Bioinspired seeding of biomaterials using three dimensional microtissues induces chondrogenic stem cell differentiation and cartilage formation under growth factor free conditions [Internet], Sci. Rep. 6 (2016 Nov 3) 36011, https://doi.org/10.1038/srep36011. Available from:.

[20] F. Wolf, C. Candrian, D. Wendt, J. Farhadi, M. Heberer, I. Martin, et al., Cartilage tissue engineering using pre-aggregated human articular chondrocytes, Eur. Cell. Mater. 16 (2008 Dec) 92–99.

[21] J. Friedrich, C. Seidel, R. Ebner, L.A. Kunz-Schughart, Spheroid-based drug screen: considerations and practical approach [Internet], Nat. Protoc. 4 (3) (2009) 309–324, https://doi.org/10.1038/nprot.2008.226. Available from:.

[22] H. Kurosawa, Methods for inducing embryoid body formation: in vitro differentiation system of embryonic stem cells [Internet], J. Biosci. Bioeng. 103 (5) (2007) 389–398. Available from: http://www.sciencedirect.com/science/article/pii/S1389172307700786.

[23] L.S. Moreira Teixeira, J.C.H. Leijten, J. Sobral, R. Jin, A.A. van Apeldoorn, J. Feijen, et al., High throughput generated micro-aggregates of chondrocytes stimulate cartilage formation in vitro and in vivo, Eur. Cell. Mater. 23 (2012 Jun) 387–399.

[24] K.Y. Lee, D.J. Mooney, Alginate: properties and biomedical applications [Internet], Prog. Polym. Sci. 37 (1) (2012 Jan) 106–126. Available from: https://www.ncbi.nlm.nih.gov/pubmed/22125349.

[25] T. Ashida, S. Sakai, M. Taya, Competing two enzymatic reactions realizing one-step preparation of cell-enclosing duplex microcapsules, Biotechnol. Prog. 29 (6) (2013) 1528–1534.

[26] T. Kamperman, S. Henke, B. Zoetebier, N. Ruiterkamp, R. Wang, B. Pouran, et al., Nanoemulsion-induced enzymatic crosslinking of tyramine-functionalized polymer droplets [Internet], J. Mater. Chem. B 5 (25) (2017) 4835–4844, https://doi.org/10.1039/C7TB00686A. Available from:.

[27] T. Kamperman, B. van Loo, M. Gurian, S. Henke, M. Karperien, J. Leijten, On-the-fly exchangeable microfluidic nozzles for facile production of various monodisperse micromaterials, Lab Chip 19 (11) (2019 Jun) 1977–1984.

[28] T. Kamperman, S. Henke, C.W. Visser, M. Karperien, J. Leijten, Centering single cells in microgels via delayed crosslinking supports long-term 3D culture by preventing cell escape, Small 13 (22) (2017) 1–10.

[29] T. Kamperman, M. Koerselman, C. Kelder, J. Hendriks, J.F. Crispim, X. de Peuter, et al., Spatiotemporal material functionalization via competitive supramolecular complexation of avidin and biotin analogs [Internet], Nat. Commun. 10 (1) (2019) 4347, https://doi.org/10.1038/s41467-019-12390-4. Available from:.

[30] S. Henke, J. Leijten, E. Kemna, M. Neubauer, A. Fery, A. van den Berg, et al., Enzymatic crosslinking of polymer conjugates is superior over ionic or UV crosslinking for the on-chip production of cell-laden microgels, Macromol. Biosci. (2016) 1524–1532.

[31] R. Jin, L.S. Moreira Teixeira, P.J. Dijkstra, C.A. van Blitterswijk, M. Karperien, J. Feijen, Chondrogenesis in injectable enzymatically crosslinked heparin/dextran hydrogels, J. Contr. Release 152 (1) (2011 May) 186–195.

[32] J.W.H. Wennink, K. Niederer, A.I. Bochyńska, L.S. Moreira Teixeira, M. Karperien, J. Feijen, et al., Injectable hydrogels by enzymatic co-crosslinking of dextran and hyaluronic acid tyramine conjugates [Internet], Macromol. Symp. 309-310 (1) (2011 Dec 15) 213–221, https://doi.org/10.1002/masy.201100032. Available from:.

[33] K.M. Park, K.S. Ko, Y.K. Joung, H. Shin, K.D. Park, In situ cross-linkable gelatin–poly(ethylene glycol)–tyramine hydrogel via enzyme-mediated reaction for tissue regenerative medicine [Internet], J. Mater. Chem. 21 (35) (2011) 13180–13187, https://doi.org/10.1039/C1JM12527C. Available from:.

[34] R. Jin, L.S. Moreira Teixeira, P.J. Dijkstra, M. Karperien, C.A. van Blitterswijk, Z.Y. Zhong, et al., Injectable chitosan-based hydrogels for cartilage tissue engineering, Biomaterials 30 (13) (2009 May) 2544–2551.

[35] S. Sakai, K. Kawakami, Synthesis and characterization of both ionically and enzymatically cross-linkable alginate, Acta Biomater. 3 (4) (2007 Jul) 495–501.

[36] S. Sakai, K. Hirose, K. Taguchi, Y. Ogushi, K. Kawakami, An injectable, in situ enzymatically gellable, gelatin derivative for drug delivery and tissue engineering [Internet], Biomaterials vol. 30 (20) (2009) 3371–3377. Available from: http://www.sciencedirect.com/science/article/pii/S0142961209003007.

[37] K.S. Lim, M.H. Alves, L.A. Poole-Warren, P.J. Martens, Covalent incorporation of non-chemically modified gelatin into degradable PVA-tyramine hydrogels, Biomaterials 34 (29) (2013 Sep) 7097–7105.

[38] L.-S. Wang, F. Lee, J. Lim, C. Du, A.C.A. Wan, S.S. Lee, et al., Enzymatic conjugation of a bioactive peptide into an injectable hyaluronic acid-tyramine hydrogel system to promote the formation of functional vasculature, Acta Biomater. 10 (6) (2014 Jun) 2539–2550.

[39] M. Gülden, A. Jess, J. Kammann, E. Maser, H. Seibert, Cytotoxic potency of H2O2 in cell cultures: impact of cell concentration and exposure time [Internet], Free Radic. Biol. Med. 49 (8) (2010) 1298–1305. Available from: http://www.sciencedirect.com/science/article/pii/S0891584910004417.

[40] M. Gulden, A. Jess, J. Kammann, E. Maser, H. Seibert, Cytotoxic potency of H2O2 in cell cultures: impact of cell concentration and exposure time, Free Radic. Biol. Med. 49 (8) (2010 Nov) 1298–1305.

[41] T. Kamperman, S. Henke, C.W. Visser, M. Karperien, J. Leijten, Centering single cells in microgels via delayed crosslinking supports long-term 3D culture by preventing cell escape [Internet], Small 13 (22) (2017 Apr 28) 1603711, https://doi.org/10.1002/smll.201603711. Available from:.

[42] T.C. Lim, W.S. Toh, L.-S. Wang, M. Kurisawa, M. Spector, The effect of injectable gelatin-hydroxyphenylpropionic acid hydrogel matrices on the proliferation, migration, differentiation and oxidative stress resistance of adult neural stem cells [Internet], Biomaterials 33 (12) (2012) 3446–3455. Available from: http://www.sciencedirect.com/science/article/pii/S0142961212000695.

[43] W.S. Toh, T.C. Lim, M. Kurisawa, M. Spector, Modulation of mesenchymal stem cell chondrogenesis in a tunable hyaluronic acid hydrogel microenvironment [Internet], Biomaterials 33 (15) (2012) 3835–3845. Available from: http://www.sciencedirect.com/science/article/pii/S0142961212001780.

[44] F. Xu, K.J.L. Burg, Three-dimensional polymeric systems for cancer cell studies [Internet]. 2007/07/31 ed, Cytotechnology 54 (3) (2007 Jul) 135–143. Available from: https://www.ncbi.nlm.nih.gov/pubmed/19003005.

[45] E. Kaemmerer, F.P.W. Melchels, B.M. Holzapfel, T. Meckel, D.W. Hutmacher, D. Loessner, Gelatine methacrylamide-based hydrogels: an alternative three-dimensional cancer cell culture system, Acta Biomater. 10 (6) (2014 Jun) 2551–2562.